An Analytical Approach to Maximum Power Tracking and Loss Minimization of a Doubly Fed Induction Generator Considering Core Loss

Bo-An Chen, Tien-Kei Lu, Yuan-Yih Hsu, *Senior Member, IEEE*, Woei-Luen Chen, *Member, IEEE*, and Zheng-Cong Lee

***Abstract*—To get maximum output power from a doubly fed induction generator (DFIG), it is essential to extract maximum mechanical power from the wind turbine and to minimize generator losses. The goal of maximum power tracking and minimum loss is usually achieved through vector control of rotor current. In other words, the *d*-axis and *q*-axis rotor currents I_{dr} and I_{qr} must be properly controlled as wind speed changes with time. In this paper, an analytical approach is developed to determine proper rotor current commands I^*_{dr} and I^*_{qr} which give maximum mechanical power and minimum loss based on the measured generator speed. The proposed analytical approach is more efficient than the exhaustive search approach proposed in a previous study and is, therefore, more suitable for real-time performance improvements. In addition, core loss component, which was usually neglected in previous studies, is included in the DFIG model in order to have more accurate results. The effectiveness of the derived analytical formulas is demonstrated by an example.**

***Index Terms*—Core loss, doubly fed induction generator (DFIG), loss minimization, maximum output power, maximum power tracking, wind energy conversion, wind turbine generator.**

I. Introduction

DOUBLY fed induction generators (DFIGs) have been widely employed for wind energy conversion since they can be operated under a wide speed range from subsynchronous to supersynchronous speeds [1]–[14]. In contrast to a synchronous generator that requires a power converter of full capacity in the stator circuit, a DFIG needs a back-to-back converter in the rotor circuit rated only about 30% of the generator capacity.

As wind speed changes with time, generator speed changes in order to extract maximum mechanical power from the wind turbine [15]. In addition, generator loss must be minimized in order to get maximum power output from the DFIG. By aligning the synchronous direct-axis (*d*-axis) to the stator flux vector [16] or stator voltage vector [17], it has been shown that maximum mechanical power can be extracted from the wind turbine if the *q*-axis component of the rotor current I_{qr} is driven to its reference value I^*_{qr} which is determined based on generator speed [16]. Loss minimization was not considered and the *d*-axis component of rotor current I^*_{dr} was set to be zero in [16]. Optimal rotor currents I^*_{dr} and I^*_{qr} that minimized total copper losses were derived by Hofmann and Okafor [18] based on steady-state equations neglecting rotor and stator resistances. Using a model based on the assumption of constant stator flux linkage, an expression for the *d*-axis rotor current I^*_{dr} which minimizes copper loss was derived in [19]. Recently, an approach based on a detailed model with stator resistance and changing stator flux linkage was presented in [20] to reach the rotor excitation voltage which maximizes DFIG output power. However, the optimal rotor excitation voltage was obtained using an exhaustive search method which is rather time consuming.

In this paper, an analytical approach is proposed to compute the optimal rotor currents I^*_{qr} and I^*_{dr} using a detailed model with stator resistance, changing stator flux linkage, and core loss. The desired rotor currents I^*_{qr} and I^*_{dr} can be solved directly by the derived analytical formulas rather than by using the exhaustive search method in [20].

The main features of this paper are summarized as follows.

1) The desired rotor current commands I^*_{qr} and I^*_{dr}, which maximize the mechanical power extracted from the wind turbine and minimize the DFIG losses, can be obtained in a more efficient manner than the exhaustive search method in [20].
2) In order to get more accurate rotor current commands, core loss component, which was neglected in previous papers, is included in the DFIG model.

II. System Model

Fig. 1 shows the system configuration for the DFIG system at the laboratory. The parameters of the 2.2-kW, 220-V, 60-Hz, six-pole machine are given in Appendix A.

As shown in Fig. 1, the induction generator is driven by a servomotor. A wind turbine simulator is implemented on a digital computer to generate the maximum mechanical power command P^*_m based on the measured generator speed ω_r. It is assumed that the maximum mechanical power is related to generator speed by the expression [16]

$$P^*_m = K_{\rm opt}\omega_r^3. \tag{1}$$

Manuscript received September 8, 2011; revised January 7, 2012; accepted March 4, 2012. Date of publication April 9, 2012; date of current version May 18, 2012. This work was supported by the National Science Council Taiwan under Contract 97-2221-E-002-256-MY3. Paper no. TEC-00468-2011.

B.-A. Chen, T.-K. Lu, and Y.-Y. Hsu are with the Department of Electrical Engineering, National Taiwan University, Taipei 106, Taiwan (e-mail: r98921017@ntu.edu.tw; r99921091@ntu.edu.tw; yyhsu@cc.ee.ntu.edu.tw).

W.-L. Chen and Z.-C. Lee are with the Department of Electrical Engineering, Chang Gung University, Taoyuan 333, Taiwan (e-mail: wlchen@mail.cgu.edu.tw; m9921027@stmail.cgu.edu.tw).

Color versions of one or more of the figures in this paper are available online at http://ieeexplore.ieee.org.

Digital Object Identifier 10.1109/TEC.2012.2190513

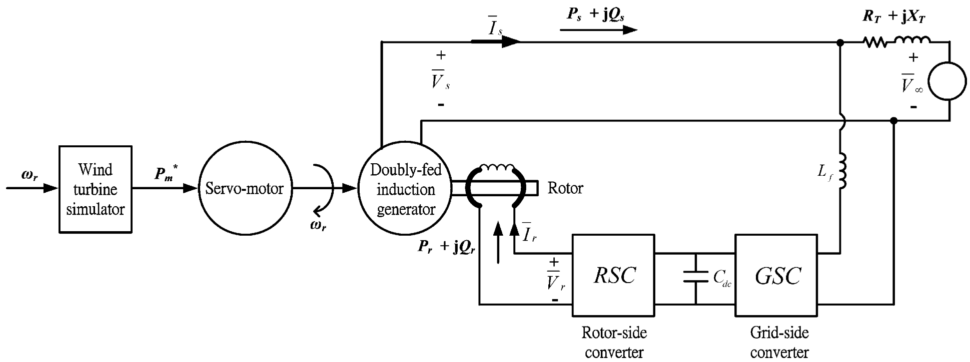

Fig. 1. System configuration for the DFIG.

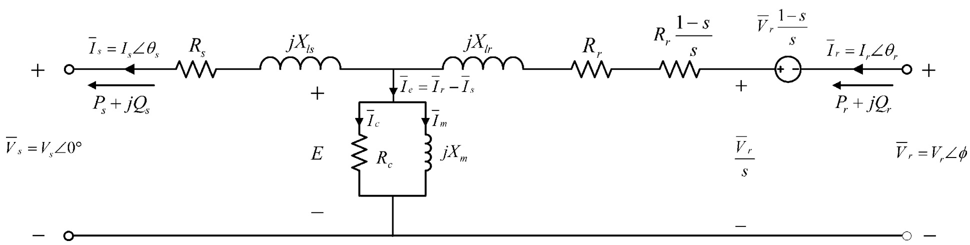

Fig. 2. Steady-state equivalent circuit for a DFIG.

When the direct-axis (*d*-axis) is aligned to stator flux linkage, the rotor voltage $\bar{V}_r$, rotor current $\bar{I}_r$, stator voltage $\bar{V}_s$, and stator current $\bar{I}_s$ can be transformed from *abc* coordinates to their *dq* components. Then, the rotor voltage $\bar{V}_r$ can be controlled by the rotor-side converter using the vector control scheme as shown in [16].

It has been shown [19] that the mechanical power extracted from the wind turbine is controlled mainly by the *q*-axis rotor current I_{qr}, while the copper loss is mainly affected by the *d*-axis rotor current I_{dr}. How to determine an optimal pair of *q*-axis and *d*-axis rotor current commands I_{qr}^* and I_{dr}^* such that the mechanical power extracted from the wind turbine can be maximized and generator losses can be minimized is of major concern in this study.

III. Analytical Formulas for Maximum Power Tracking and Loss Minimization

Fig. 2 depicts the steady-state equivalent circuit for a DFIG [5], [15], [20].

The symbols used in Fig. 2 are defined as follows:

$\bar{\lambda}_s = \lambda_s \angle\theta_{fs}$ stator flux linkage;
$\bar{V}_s = V_s\angle 0^\circ$ stator voltage;
$\bar{V}_r = V_r\angle\phi$ rotor excitation voltage;
$\bar{I}_s = I_s\angle\theta_s$ stator current;
$\bar{I}_r = I_r\angle\theta_r$ rotor current;
$\bar{I}_e$ exciting current;
$\bar{I}_m$ magnetizing current;
$\bar{I}_c$ core loss component of $\bar{I}_e$;
R_s stator resistance;
R_r rotor resistance;
X_{ls} stator leakage reactance;
X_{lr} rotor leakage reactance;
X_m magnetizing reactance;
R_c core loss resistance;
$s = (\omega_s - \omega_r)/\omega_s$ slip;
ω_s stator synchronous speed;
ω_r rotor speed.

The desired rotor current $\bar{I}_r$ with maximum extracted mechanical power and minimum copper loss can be computed using the following steps that are summarized by the flowchart in Appendix B.

Step1: Express stator current $\bar{I}_s$ in terms of rotor current $\bar{I}_r$ and stator voltage $\bar{V}_s$.

The voltage equation for the stator is first written as

$$\bar{V}_s = Z_m \bar{I}_e - (R_s + jX_{ls})\bar{I}_s \tag{2}$$

where

$$Z_m = R_c||(jX_m) = \frac{R_c X_m}{R_c^2 + X_m^2}(X_m + jR_c)$$

$$\bar{I}_e = \bar{I}_r - \bar{I}_s.$$

As shown in Fig. 3, the real axis *R* is aligned to stator voltage $\bar{V}_s$ since $\bar{V}_s = V_s\angle 0^\circ$ is taken as the angle reference. The rotor current $\bar{I}_r$ and stator current $\bar{I}_s$ can be expressed using their real axis$^{(R)}$ and imaginary axis$^{(I)}$ components as $\bar{I}_r = I_r^R + jI_r^I$ and $\bar{I}_s = I_s^R + jI_s^I$, respectively.

By separating real and imaginary parts of (2), we obtain

$$\begin{aligned} &-(B_2R_s + A_2X_m)I_s^R + (B_2X_{ls} + A_2R_c)I_s^I \\ &\quad = -A_2X_m I_r^R + A_2R_c I_r^I + B_2V_s \end{aligned} \tag{3}$$

$$\begin{aligned} &(B_2X_{ls} + A_2R_c)I_s^R + (B_2R_s + A_2X_m)I_s^I \\ &\quad = A_2R_c I_r^R + A_2X_m I_r^I \end{aligned} \tag{4}$$

where $A_2 = R_c X_m$ and $B_2 = R_c^2 + X_m^2$.

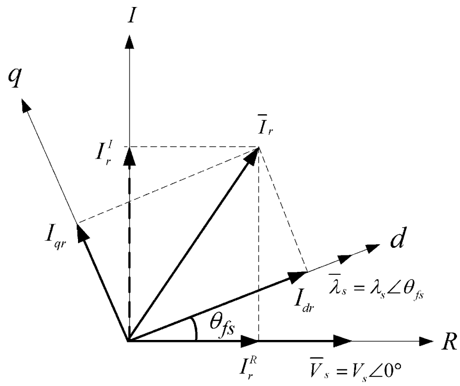

Fig. 3. Coordinate transformation between real (*R*) and imaginary (*I*) axes and *dq* axes.

From (3) and (4), the stator current components $I_s{}^R$ and $I_s{}^I$ can be expressed in terms of rotor current components $I_r{}^R$ and $I_r{}^I$ as follows:

$$I_s^R = \frac{1}{C_2}(D_2 I_r^R - E_2 I_r^I + F_2) \quad (5)$$

$$I_s^I = \frac{1}{C_2}(E_2 I_r^R + D_2 I_r^I + G_2) \quad (6)$$

where $C_2 = (B_2 R_s + A_2 X_m)^2 + (B_2 X_{ls} + A_2 R_c)^2$, $D_2 = A_2 B_2 (A_2 + R_c X_{ls} + R_s X_m)$, $E_2 = A_2 B_2 (R_c R_s - X_m X_{ls})$, $F_2 = -B_2 V_s (B_2 R_s + A_2 X_m)$, and $G_2 = B_2 V_s (B_2 X_{ls} + A_2 R_c)$.

Step2: Derive formulas for stator powers P_s and Q_s, rotor powers P_r and Q_r, copper loss P_{cu}, and core loss P_{core} in terms of rotor current components I_r^R and I_r^I.

Stator powers P_s and Q_s can be expressed as

$$\begin{aligned} P_s &= 3\mathrm{Re}(\bar{V}_s \bar{I}_s^*) \\ &= 3 V_s I_s^R \\ &= 3\frac{V_s}{C_2}(D_2 I_r^R - E_2 I_r^I + F_2) \end{aligned} \quad (7)$$

$$\begin{aligned} Q_S &= 3\mathrm{Im}(V_S I_S^*) \\ &= 3 V_S I_S^I \\ &= 3 V_S \frac{1}{C_2}(E_2 I_r^R + D_2 I_r^I + G_2). \end{aligned} \quad (8)$$

To derive the formula for rotor power P_r, let us first write down the rotor voltage equation from Fig. 3

$$\frac{\bar{V}_r}{s} = \bar{V}_s + (R_s + jX_{ls})\bar{I}_s + \left(\frac{R_r}{s} + jX_{lr}\right)\bar{I}_r. \quad (9)$$

By substituting (5) and (6) into (9) and rearranging, we get

$$\begin{aligned} \bar{V}_r &= V_r^R + jV_r^I \\ &= \left[\left(\frac{s}{C_2}H_2 + R_r\right) I_r^R - \left(\frac{s}{C_2}I_2 + sX_{lr}\right) I_r^I + \frac{D_2}{C_2} sV_s\right] \\ &\quad + j\left[\left(\frac{s}{C_2}I_2 + sX_{lr}\right) I_r^R + \left(\frac{s}{C_2}H_2 + R_r\right) I_r^I + \frac{s}{C_2}K_2\right] \end{aligned} \quad (10)$$

where

$$\begin{aligned} H_2 &= A_2 B_2 [A_2 R_s + X_m (R_s^2 + X_{ls}^2)] \\ I_2 &= A_2 B_2 [A_2 X_{ls} + R_c (R_s^2 + X_{ls}^2)] \\ K_2 &= A_2 B_2 V_s (R_c R_s - X_m X_{ls}). \end{aligned}$$

Then, the rotor powers can be computed as

$$\begin{aligned} P_r &= 3\mathrm{Re}(\bar{V}_r \bar{I}_r^*) \\ &= 3(V_r^R I_r^R + V_r^I I_r^I) \\ &= 3\left\{L_2[(I_r^R)^2 + (I_r^I)^2] + \frac{D_2}{C_2} sV_s I_r^R + \frac{s}{C_2} K_2 I_r^I\right\} \end{aligned} \quad (11)$$

where

$$\begin{aligned} L_2 &= \frac{s}{C_2} H_2 + R_r \\ Q_r &= 3\mathrm{Im}(\bar{V}_r \bar{I}_r^*) \\ &= 3(V_r^R I_r^I + V_r^I I_r^R) \\ &= 3\left[\left(\frac{s}{C_2}H_2 + R_r\right) I_r^R \right. \\ &\quad \left. - \left(\frac{s}{C_2}I_2 + sX_{lr}\right) I_r^I + \frac{D_2}{C_2} sV_S\right] I_r^I \\ &\quad + 3\left[\left(\frac{s}{C_2}I_2 + sX_{lr}\right) I_r^R \right. \\ &\quad \left. + \left(\frac{s}{C_2}H_2 + R_r\right) I_r^I + \frac{s}{C_2}K_2\right] I_r^R. \end{aligned} \quad (12)$$

The copper loss P_{cu} can be expressed in terms of I_r^R and I_r^I as follows:

$$\begin{aligned} P_{\mathrm{cu}} &= 3[(I_s^R)^2 + (I_s^I)^2] R_s + 3[(I_r^R)^2 + (I_r^I)^2] R_r \\ &= \frac{3}{C_2^2}\{M_2[(I_r^R)^2 + (I_r^I)^2] + N_2 I_r^R + P_2 I_r^I + Q_2\} \end{aligned} \quad (13)$$

where

$$\begin{aligned} M_2 &= (D_2^2 + E_2^2) R_s + C_2^2 R_r \\ N_2 &= 2(E_2 G_2 + D_2 F_2) R_s \\ P_2 &= 2(D_2 G_2 - E_2 F_2) R_s \\ Q_2 &= (F_2^2 + G_2^2) R_s. \end{aligned}$$

To derive the core loss, let us first compute the core loss current as

$$\begin{aligned} \bar{I}_c &= I_c^R + jI_c^I \\ &= \frac{\bar{E}}{R_c} \\ &= \frac{1}{R_c}[\bar{V}_s + (R_s + jX_{ls})\bar{I}_s]. \end{aligned} \quad (14)$$

Then, the core loss can be computed as

$$\begin{aligned} P_{\text{core}} &= 3[(I_c^R)^2 + (I_c^I)^2]R_c \\ &= \frac{3}{R_c C_2^2}\{R_2(D_2^2+E_2^2)[(I_r^R)^2 + (I_r^I)^2] \\ &\quad + T_2 I_r^R + U_2 I_r^I + V_2\} \end{aligned} \tag{15}$$

where

$$\begin{aligned} R_2 &= R_s^2 + X_{ls}^2 \\ T_2 &= \frac{N_2}{R_s}R_2 + 2C_2V_s(D_2R_s - E_2X_{ls}) \\ U_2 &= \frac{P_2}{R_s}R_2 - 2C_2V_s(E_2R_s + D_2X_{ls}) \\ V_2 &= \frac{Q_2}{R_s}R_2 + 2C_2V_s(F_2R_s - G_2X_{ls}) + C_2^2V_s^2. \end{aligned}$$

Step3: Derive the first formula for solving I_r^R and I_r^I based on maximum extracted mechanical power.

In order for the DFIG to extract maximum mechanical power from the wind turbine, the total output power $P_s - P_r$ must be equal to the maximum mechanical power P_m^* in (1) minus the copper loss P_{cu} and core loss P_{core}. In other words, we have the first formula for solving I_r^R and I_r^I

$$\begin{aligned} P_m^* &= K_{\text{opt}}\omega_r^3 \\ &= P_s - P_r + P_{\text{cu}} + P_{\text{core}} \\ &= W_2(I_r^R)^2 + W_2(I_r^I)^2 + X_2I_r^R + Y_2I_r^I + Z_2 \end{aligned} \tag{16}$$

where

$$\begin{aligned} W_2 &= \frac{3}{C_2^2}\left[-C_2^2L_2 + M_2 + \frac{R_2(D_2^2+E_2^2)}{R_c}\right] \\ X_2 &= \frac{3}{C_2^2}\left[C_2D_2V_s(1-s) + N_2 + \frac{T_2}{R_c}\right] \\ Y_2 &= \frac{3}{C_2^2}\left(-C_2E_2V_s - C_2K_2s + P_2 + \frac{U_2}{R_c}\right) \\ Z_2 &= \frac{3}{C_2^2}\left(C_2F_2V_s + Q_2 + \frac{V_2}{R_c}\right). \end{aligned}$$

Step4: Derive the second formula for solving I_r^R and I_r^I based on loss minimization.

To achieve minimum loss, let us take the partial derivative of the loss P_{cu} with respect to I_r^R and get the following formula:

$$\frac{\partial(P_{\text{cu}} + P_{\text{core}})}{\partial I_r^R} = 0. \tag{17}$$

Since P_{cu} and P_{core} are functions of I_r^I as well as I_r^R, we need $\partial I_r^I/\partial I_r^R$ in order to solve (17). Fortunately, we can take the partial derivative of (16) with respect to I_r^R and get the desired $\partial I_r^I/\partial I_r^R$ as follows:

$$\frac{\partial I_r^I}{\partial I_r^R} = -\frac{2W_2I_r^R + X_2}{2W_2I_r^I + Y_2}. \tag{18}$$

Substituting (18) into (17), we get

$$A'I_r^R + B'I_r^I + C' = 0 \tag{19}$$

where

$$\begin{aligned} A' &= 2Y_2[M_2R_c + R_2(D_2^2+E_2^2)] - 2W_2(P_2R_c + U_2) \\ B' &= -2X_2[M_2R_c + R_2(D_2^2+E_2^2)] + 2W_2(N_2R_c + T_2) \\ C' &= Y_2(N_2R_c + T_2) - X_2(P_2R_c + U_2). \end{aligned}$$

From (19), we obtain the second formula for solving I_r^R and I_r^I

$$I_r^I = \frac{A'I_r^R + C'}{B'}. \tag{20}$$

Step5: Solve I_r^R and I_r^I using (16) and (20).

When I_r^I in (20) is substituted into (16), the following equation is reached:

$$D'(I_r^R)^2 + E'I_r^R + F' = 0 \tag{21}$$

where

$$\begin{aligned} D' &= W_2 + W_2\frac{(A')^2}{(B')^2} \\ E' &= W_2\frac{2A'C'}{(B')^2} + X_2 - Y_2\frac{A'}{B'} \\ F' &= W_2\frac{(C')^2}{(B')^2} - Y_2\frac{C'}{B'} + Z_2 - P_m^*. \end{aligned}$$

The desired rotor current I_r^R can be computed as

$$I_r^R = \frac{-E' \pm \sqrt{(E')^2 - 4D'F'}}{2D'}. \tag{22}$$

I_r^I can then be solved using (20). The pair of solutions I_r^R and I_r^I in (22) and (20) with less loss are the desired rotor current components in real and imaginary axes.

Step6: Compute the desired I_{dr} and I_{qr} from I_r^R and I_r^I.

As shown in Fig. 3, the *d*-axis is aligned to the stator flux linkage $\bar{\lambda}_s = \lambda_s\angle\theta_{fs}$ which is computed using the following equation:

$$j\omega_s\bar{\lambda}_s = \bar{V}_s + \bar{I}_sR_s. \tag{23}$$

From Fig. 3, the desired rotor current components I_{dr} and I_{qr} can be derived from I_r^R and I_r^I

$$I_{dr} = I_r^R\cos\theta_{fs} + I_r^I\sin\theta_{fs} \tag{24}$$

$$I_{qr} = -I_r^R\sin\theta_{fs} + I_r^I\cos\theta_{fs}. \tag{25}$$

IV. Example

To demonstrate the effectiveness of the derived analytical formulas for rotor currents I_{dr} and I_{qr}, the performance of DFIG in Fig. 1 with the parameters in Appendix A was examined.

A. DFIG Model Without Core Loss

When the core loss component was neglected, the optimal *d*-axis and *q*-axis rotor current components I_{dr}^* and I_{qr}^* with maximum extracted mechanical power and minimum loss were computed as functions of slip using analytical formulas in Appendix C. With the rotor currents at hand, we proceeded to compute stator real power P_s, rotor real power P_r, output power

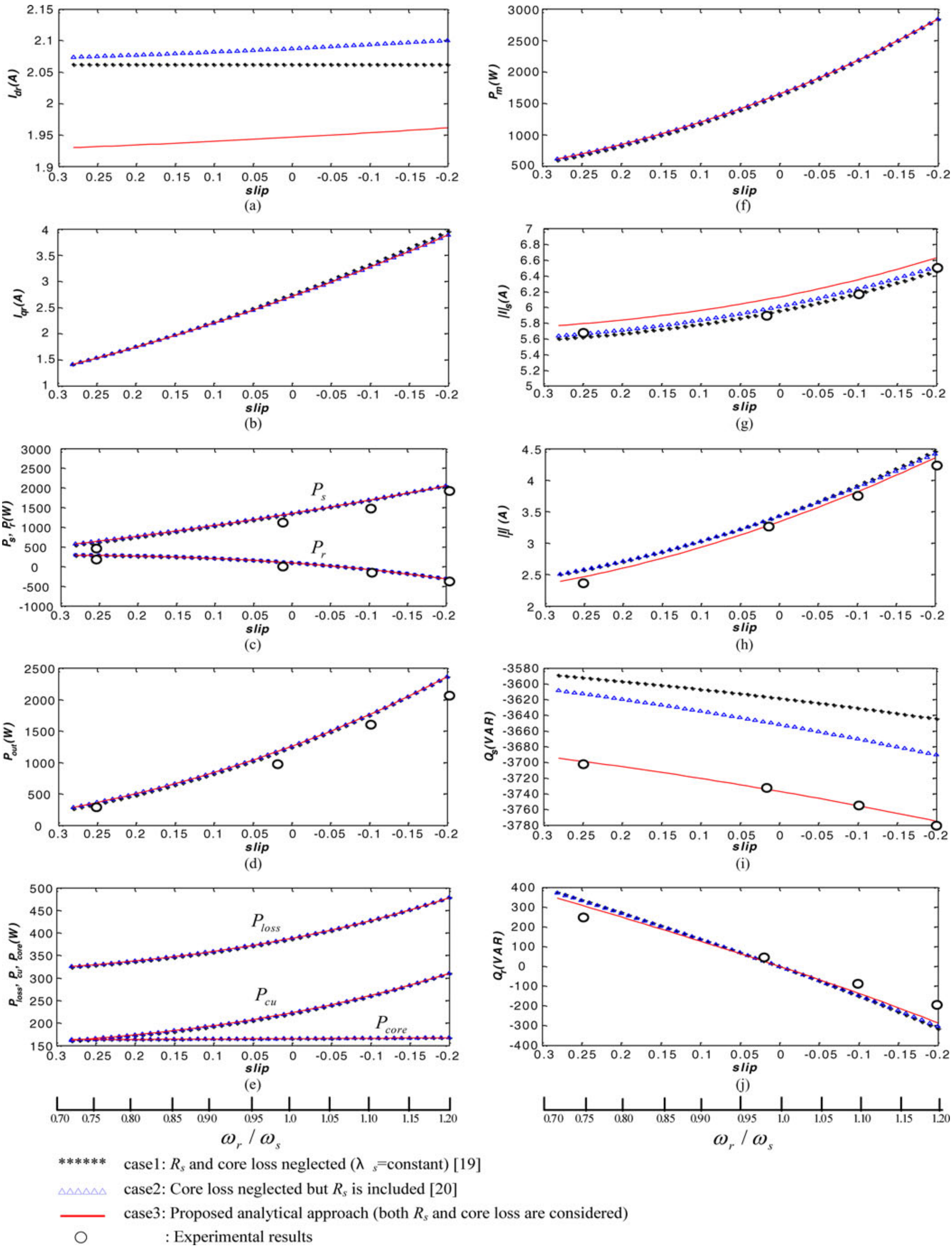

Fig. 4. Optimal d-axis and q-axis rotor commands and output powers for the DFIG model with core loss. (a) Optimal d-axis rotor current. (b) Optimal q-axis rotor current. (c) Stator real power and rotor real power. (d) Output power. (e) Loss. (f) Mechanical power. (g) Stator current. (h) Rotor current. (i) Stator reactive power. (j) Rotor reactive power.

$P_{\rm out}$ (=$P_s - P_r$), loss $P_{\rm loss}$ (= $P_{\rm cu}$), mechanical power P_m ($P_{\rm out}$+$P_{\rm loss}$), stator current I_s, rotor current I_r, stator reactive power Q_s, and rotor reactive power Q_r, as depicted in Fig. 4.

It took less than 1 s for the proposed analytical approach to reach the desired solution, while it took about 5 min for the exhaustive search method [20] to get similar solutions. It is, thus, concluded that the same results can be reached by the proposed analytical formulas in a much more efficient manner than the exhaustive search method.

B. DFIG Model With Core Loss

When the core loss component is included in the DFIG model, the optimal rotor current commands I^*_{dr} and I^*_{qr} were determined using (20), (22), (24), and (25). The resulting currents and powers are depicted in Fig. 4.

For purpose of comparison, the following three cases were considered.

Case1: The rotor current commands I^*_{dr} and I^*_{qr} were determined based on the assumptions of zero stator resistance and zero core loss [19]. Then, the powers were computed using these rotor current commands and the DFIG model with stator resistance and core loss.

Case2: The rotor current commands I^*_{dr} and I^*_{qr} were determined based on the assumption of zero core loss [20]. Then, the powers were computed using these rotor current commands and the DFIG model with stator resistance and core loss.

Case3: The rotor current commands I^*_{dr} and I^*_{qr} were determined using the analytical formulas (20), (22), (24), and (25) in this paper for the complete DFIG model with stator resistance and core loss. Then, the powers were computed using these rotor current commands and the DFIG model with stator resistance and core loss.

Based on the results in Fig. 4, the following observations can be made.

1) It is observed from the results in Fig. 4(a) that, in case 1 where R_s was neglected and λs was assumed to remain constant, the optimal *d*-axis rotor current I_{dr} remains unchanged as generator speed changes [19]. When R_s was included in cases 2 [20] and 3, the optimal *d*-axis rotor current I_{dr} changes with generator speed.
2) It is also observed from Fig. 4(a) that the optimal *d*-axis rotor currents for the three cases are quite different.
3) As shown in Fig. 4(b), case 1 gives slightly larger *q*-axis rotor current command I_{qr} than case 2. It is also observed from Fig. 4(b) that the *q*-axis rotor current command in case 2 is very close to that in case 3.
4) It is observed from the curves in Fig. 4(c)–(f) that the real powers for the three cases differ not much from one another. This is due to the fact that the real powers of a DFIG are mainly affected by the *q*-axis rotor currents I_{qr} [19] which differ not much as shown in Fig. 4(b). On the other hand, the reactive powers in Fig. 4(i) and (j), which are mainly controlled by the *d*-axis rotor currents I_{dr}, differ much for the three cases, as the *d*-axis rotor currents for the three cases are quite different as shown in Fig. 4(a).
5) It is also observed from the curves in Fig. 4 that the experimental results match closely to the analytical results in case 3.

V. Conclusion

Analytical formulas have been derived for the computation of *d*-axis and *q*-axis rotor current commands for a DFIG which give maximum extracted mechanical power and minimum generator loss. Both the DFIG model without core loss and with core loss have been investigated. Specific conclusions are as follows.

1) The proposed analytical approach is much more efficient than the exhaustive search method in a previous study since the desired rotor current commands I_{dr} and I_{qr} can be computed directly by using the derived analytical formulas. As a result, the analytical approach can be used to adjust the rotor current commands in real-time based on online measured generator speed.
2) Core loss component, which was usually neglected in previous studies, has been taken into account in the DFIG model in order to get more accurate rotor current commands.
3) For small wind turbine generators, core loss component has significant impacts on *d*-axis rotor current command I_{dr} and stator and rotor reactive powers Q_s and Q_r. However, it has only minor effects on *q*-axis rotor current command I_{qr} since the mechanical power P_m is related to I_{qr} by the expression [16]

$$P_m = \omega_r T_{em} = \omega_r \left(\frac{3}{2}\frac{P}{2}\frac{L_m}{L_S}\lambda_{ds} I_{qr}\right).$$

Therefore, inclusion of core loss component in the derivation of rotor commands has only minor effect on total extracted power.
4) Rotor current commands and real and reactive powers are affected by stator resistance to a great extent, especially for small generators. It is, thus, desirable to include stator resistance in the DFIG model in order to get more accurate results.
5) The rotor current commands derived in this paper can only be applied to maximum output power tracking mode. When the wind velocity is high and the current commands exceed the rated values, the DFIG must be operated at the rated output power mode [20].

Appendix A

Nameplate data of the DFIG:

Three-phase, 60-Hz, Y-connected, six poles;

Stator: 220 V/phase, 6.9 A;

Rotor: 70 V/phase, 6.9 A;

Machine parameters: $V_s = 216$ V; $R_s = 1.14\ \Omega$; $R_r = 2.818\ \Omega$; $X_{ls} = 2.21\ \Omega$; $X_{lr} = 2.21\ \Omega$; $X_m = 26.9\ \Omega$;

Turn ratio (N_s / N_r) = 5.67:1;

(R_r, X_{lr}, and X_m are referred to the stator).

APPENDIX B

The flowchart for the procedures to derive the derived rotor current $\bar{I}_r$.

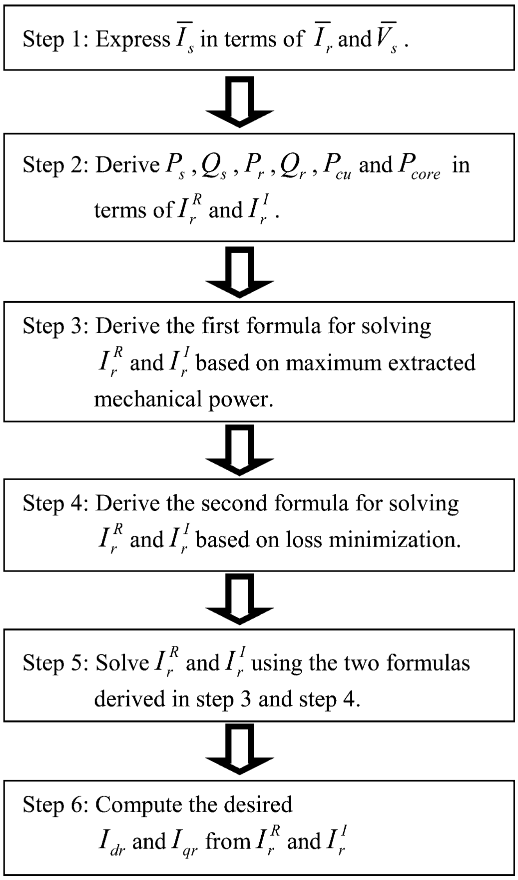

APPENDIX C

Detailed procedures for deriving the analytical formulas for the model without core loss are exactly the same as those for the model with core loss. Therefore, these procedures are omitted and only the results are presented.

Equations (5) and (6) are modified as

$$I_S^R = \frac{1}{A_1}(B_1 I_r^R - C_1 I_r^I + D_1) \tag{A1}$$

$$I_S^I = \frac{1}{A_1}(C_1 I_r^R + B_1 I_r^I + E_1) \tag{A2}$$

where

$$\begin{aligned} A_1 &= R_S^2 + X_S^2 \\ B_1 &= X_m X_S \\ C_1 &= R_S X_m \\ D_1 &= -R_S V_S \\ E_1 &= X_S V_S. \end{aligned}$$

The stator powers in (7) and (8) are modified as

$$P_S = 3\frac{V_S}{A_1}(B_1 I_r^R - C_1 I_r^I + D_1) \tag{A3}$$

$$Q_S = 3\frac{V_S}{A_1}(C_1 I_r^R + B_1 I_r^I + E_1). \tag{A4}$$

The rotor powers in (11) and (12) are modified as

$$P_r = 3\left\{J_1[(I_r^R)^2 + (I_r^I)^2] + \frac{B_1}{A_1}sV_S I_r^R + \frac{s}{A_1}I_1 I_r^R\right\} \tag{A5}$$

where

$$\begin{aligned} J_1 &= \frac{s}{A_1}F_1 + R_r. \\ Q_r &= 3\left[\left(\frac{s}{A_1}F_1 + R_r\right)I_r^R \right. \\ &\quad \left. - \left(\frac{s}{A_1}G_1 + sX_{lr}\right)I_r^I + \frac{B_1}{A_1}sV_S\right]I_r^I \\ &\quad + 3\left[\left(\frac{s}{A_1}G_1 + sX_{lr}\right)I_r^R \right. \\ &\quad \left. + \left(\frac{s}{A_1}F_1 + R_r\right)I_r^I + \frac{s}{A_1}I_1\right]I_r^R \end{aligned} \tag{A6}$$

where

$$\begin{aligned} F_1 &= R_S X_m^2 \\ G_1 &= X_m(R_S^2 + X_S X_{ls}) \\ H_1 &= -V_S(R_S^2 + X_S X_{ls}) \\ I_1 &= C_1 V_S. \end{aligned}$$

The copper loss in (13) is modified as

$$P_{\text{cu}} = \frac{3}{A_1}\{(F_1 + A_1 R_r)[(I_r^R)^2 + (I_r^I)^2] + 2I_1 I_r^I + R_S V_S^2\}. \tag{A7}$$

The first formula for solving I_r^R and I_r^I in (16) is modified as

$$\begin{aligned} P_m^* &= K_{\text{opt}}\omega_r^3 = P_S - P_r + P_{\text{cu}} \\ &= K_1(I_r^R)^2 + K_1(I_r^I)^2 + L_1 I_r^R + M_1 I_r^I \end{aligned} \tag{A8}$$

where

$$\begin{aligned} K_1 &= \frac{3}{A_1}F_1(1-s) \\ L_1 &= \frac{3}{A_1}B_1 V_S(1-s) \\ M_1 &= \frac{3}{A_1}I_1(1-s). \end{aligned}$$

The second formula for solving I_r^R and I_r^I in (20) is modified as

$$I_r^I = \frac{N_1 I_r^R - I_1 L_1}{P_1} \tag{A9}$$

where

$$\begin{aligned} N_1 &= M_1(F_1 + A_1 R_r) - 2I_1 K_1 \\ P_1 &= L_1(F_1 + A_1 R_r). \end{aligned}$$

Finally, the desired solution I_r^R can be computed using the following equation:

$$I_r^R = \frac{-R_1 \pm \sqrt{R_1^2 - 4Q_1T_1}}{2Q_1}. \tag{A10}$$

Then, the imaginary axis rotor current component I_r^I is computed using (A9) and the *d*-axis and *q*-axis rotor current components can be determined using (24) and (25).

References

[1] Z. M. Salameh and L. F. Kazda, "Analysis of the steady state performance of the double output induction generator," *IEEE Trans. Energy Convers.*, vol. 1, no. 1, pp. 26–32, Mar. 1986.

[2] G. A. Smith and V. A. Nigim, "Wind-energy recovery by a static Scherbius induction generator," *IEE Proc. Generat. Transmiss. Distrib.*, vol. 128, no. 6, pp. 317–324, Nov. 1981.

[3] M. S. E. Vicatos and J. A. Tegopoulos, "Steady state analysis of a doubly-fed induction generator under synchronous operation," *IEEE Trans. Energy Convers.*, vol. 4, no. 3, pp. 495–501, Sep. 1989.

[4] H. Banakar, C. Luo, and B. T. Ooi, "Steady-state stability analysis of doubly-fed induction generator under decoupled P-Q control," *IEE Proc. Elect. Power Appl.*, vol. 153, no. 2, pp. 300–306, Mar. 2006.

[5] I. Boldea, *Variable Speed Generators*. Boca Raton, FL: CRC Press, 2006.

[6] A. Petersson, T. Thiringer, L. Harnefors, and T. Petru, "Modeling and experimental verification of grid interaction of a DFIG wind turbine," *IEEE Trans. Energy Convers.*, vol. 20, no. 4, pp. 878–886, Dec. 2005.

[7] B. C. Rabelo, Jr., W. Hofmann, J. L. da Silva, R. G. de Oliveira, and S. R. Silva, "Reactive power control design in doubly fed induction generators for wind turbines," *IEEE Trans. Ind. Electron.*, vol. 56, no. 10, pp. 4154–4162, Oct. 2009.

[8] S. Engelhardt, I. Erlich, C. Feltes, J. Kretschmann, and F. Shewarega, "Reactive power capability of wind turbines based on doubly-fed induction generators," *IEEE Trans. Energy Convers.*, vol. 26, no. 1, pp. 364–372, Mar. 2011.

[9] O. Abdel-Baqi and A. Nasiri, "Series voltage compensation for DFIG wind turbine low-voltage ride-through solution," *IEEE Trans. Energy Convers.*, vol. 26, no. 1, pp. 272–280, Mar. 2011.

[10] G. Tsourakis, B. M. Nomikos, and C. D. Vournas, "Contribution of doubly fed wind generators to oscillation damping," *IEEE Trans. Energy Convers.*, vol. 24, no. 3, pp. 783–791, Sep. 2009.

[11] J. M. Mauricio, A. E. Leon, A. Gomez-Exposito, and J. A. Solsona, "An adaptive nonlinear controller for DFIM-based wind energy conversion systems," *IEEE Trans. Energy Convers.*, vol. 23, no. 4, pp. 1025–1035, Dec. 2008.

[12] R. Pena, J. C. Clare, and G. M. Asher, "Doubly fed induction generator using back-to-back PWM converters supplying an isolated load from a variable speed wind turbine," *IEE Proc. Elect. Power Appl.*, vol. 143, no. 5, pp. 380–387, Sep. 1996.

[13] M. Kayikci and J. V. Milanovic, "Reactive power control strategies for DFIG-based plants," *IEEE Trans. Energy Convers.*, vol. 22, no. 2, pp. 389–396, Jun. 2007.

[14] D. Aguglia, P. Viarouge, R. Wamkeue, and J. Cros, "Analytical determination of steady-state converter control laws for wind turbines equipped with doubly fed induction generators," *IET Renew. Power Generat.*, vol. 2, no. 1, pp. 16–25, Mar. 2008.

[15] I. Cadirci and M. Ermis, "Double-output induction generator operating at subsynchronous and supersynchronous speeds: Steady-state performance optimization and wind-energy recovery," *IEE Proc. Elect. Power Appl.*, vol. 139, no. 5, pp. 429–442, Sep. 1992.

[16] R. Pena, J. C. Clare, and G. M. Asher, "Doubly fed induction generator using back-to-back PWM converters and its application to variable-speed wind-energy generation," *IEE Proc. Elect. Power Appl.*, vol. 143, no. 3, pp. 231–241, May 1996.

[17] S. Chondrogiannis and M. Barnes, "Stability of doubly-fed induction generator under stator voltage orientated vector control," *IET Renew. Power Generat.*, vol. 2, no. 3, pp. 170–180, Sep. 2008.

[18] W. Hofmann and F. Okafor, "Doubly-fed full-controlled induction wind generator for optimal power utilization," in *Proc. 4th IEEE Int. Conf. Power Electron. Drive Syst.*, vol. 1, Bali, Indonesia, Oct. 2001, pp. 355–361.

[19] Y. Tang and L. Xu, "A flexible active and reactive power control strategy for a variable speed constant frequency generating system," *IEEE Trans. Power Electron.*, vol. 10, no. 4, pp. 472–478, Jul. 1995.

[20] C. H. Liu and Y. Y. Hsu, "Effect of rotor excitation voltage on steady-state stability and maximum output power of a doubly fed induction generator," *IEEE Trans. Ind. Electron.*, vol. 58, no. 4, pp. 1096–1109, Apr. 2011.

Bo-An Chen received the B.S. degree from National Sun Yat-sen University, Kaohsiung, Taiwan, and the M.S. degree from National Taiwan University, Taipei, Taiwan.

His research interests include power quality, modern control, and power system analysis.

Tien-Kei Lu received the B.S. degree from the National Taiwan University of Science and Technology, Taipei, Taiwan. He is currently working toward the M.S. degree at National Taiwan University, Taipei.

His research interests include power electronics, power system analysis, and modern control.

Yuan-Yih Hsu (SM'89) was born in Taiwan on June 19, 1955. He received the B.S., M.S., and Ph.D. degrees from National Taiwan University, Taipei, Taiwan, all in electrical engineering.

Since 1977, he has been with National Taiwan University, where he is currently a Professor. His current research interests include reactive power compensation and the application of power electronics to power systems.

Dr. Hsu was elected as one of the Ten Outstanding Young Engineers by the Chinese Institute of Engineers in 1989. He is the recipient of Distinguished Research Awards from the National Science Council during 1986–1995.

Woei-Luen Chen (S'02–M'05) received the M.S.E.E. and Ph.D. degrees from National Taiwan University, Taipei, Taiwan, in 1997 and 2006, respectively.

Since 2006, he has been with the Department of Electrical Engineering, Chang Gung University, Taoyuan, Taiwan, where he is currently an Associate Professor. His current research interests include power electronic applications, reactive power compensation systems, and wind energy conversion systems.

Zheng-Cong Lee received the B.S.E.E. degree from National Ilan University, Ilan, Taiwan, in 2010. He is currently working toward the M.Sc. degree in electrical engineering at Chang Gung University, Taoyuan, Taiwan.

His research interests include power electronic applications and wind energy conversion systems.